Title
Magnetic Resonance Imaging of the Hindfoot

Journal
Foot & Ankle International, 10(1)

ISSN
1071-1007

Authors
Crim, Julia R
Cracchiolo, Andrea
Bassett, Lawrence W
et al.

Publication Date
1989-08-01

DOI
10.1177/107110078901000101

Peer reviewed

0198-0211/89/1001-0001$02.00/0
FOOT & ANKLE

Magnetic Resonance Imaging of the Hindfoot

Julia R. Crim, M.D.,*† Andrea Cracchiolo, M.D.,‡ Lawrence W. Bassett, M.D.,* Leanne L. Seeger, M.D.,*
Charles A. Soma, M.D.§ and Anne Chatelaine, M.D.‡
Los Angeles, California

ABSTRACT

This article demonstrates normal anatomy of the foot and ankle as visualized with magnetic resonance imaging (MRI) in the sagittal, axial, and coronal planes. Additionally, selected cases chosen from our experience with more than 100 clinical scans are shown to highlight the primary areas in which we have found MRI to be clinically useful: bone marrow abnormalities, especially osteomyelitis and osteonecrosis, soft tissue injuries and masses, and cases in which metallic fixators make CT evaluation problematic.

Magnetic resonance imaging (MRI) has proven its utility in the evaluation of the musculoskeletal system because of its unrivaled ability to allow soft tissue structures and bone marrow to be visualized and to image in multiple planes. These capabilities are useful in the foot and ankle, where soft tissue injury is common and the complex anatomy is more readily understood with multiplanar imaging. MRI is also noninvasive and does not use ionizing radiation, as compared with tenosynography and arthrography. Diagnostic scans can frequently be obtained despite the presence of metallic devices. Clinical experience in imaging the foot and ankle with MRI is still limited.[3,4,6,8] In this article, relevant normal anatomy in the sagittal, coronal, and axial planes is described and representative pathologic cases in which MRI provided useful clinical information are presented. Because the MRI appearance of forefoot abnormalities has been described elsewhere,[6,8] we have not included abnormalities from this region.

Full interpretation of MRI requires a basic understanding of the factors that create an MRI signal. Clinical MRI exploits the paramagnetic properties of hydrogen ions (protons). The patient is placed in a strong, static magnetic field (generally between 0.15 and 1.5 Tesla), with which mobile hydrogen ions become aligned. A short radio-frequency pulse is then superimposed on the static field, which reorients the protons. As they realign with the vector along the main magnetic field, energy is emitted and this energy is translated into an image. With spin echo imaging, the intensity of the signal, or whiteness of a tissue, depends on the density of mobile protons, the binding of the protons to macromolecules, the presence of paramagnetic and ferromagnetic substances, and the parameters used to obtain the signal: echo time and repetition time. These parameters determine the amount of T1- or T2-"weighting" of an image. In Table 1, the relative signal intensities of various tissues in the musculoskeletal system are shown. T1-weighted images, because of the contrast between fat (white) and muscle (intermediate), are superior in defining anatomy. Bone marrow pathology is also well seen on T1-weighted images, because the white signal of fatty marrow is replaced by intermediate signal due to increased fluid content. On T2-weighted images, fluid, tumor, infection, and inflammation all appear white.

MATERIAL AND METHODS

Scanning was performed with a 0.3 Tesla Fonar MRI system. Slices were 5 mm in thickness and were obtained at 5.5- or 7-mm intervals. Two signal averages were used, with a 256 × 256-imaging matrix and field of view between 21 and 25 cm, for a pixel size of 0.75 to 1 mm. A surface coil designed for head imaging provided good resolution and allowed us to scan both feet at once. For defining normal anatomy, T1-weighted images (SE TE28/TR300-800) were obtained. Pathologic cases were supplemented with T2-weighted (SE TE56/TR2000) scans as needed. In one case, a sequence designed to increase the difference in signal between fat and water ("spin echo phase contrast" scan) was performed to enhance visualization of suspected marrow abnormality (case 3).

* Department of Diagnostic Radiology, UCLA School of Medicine, Los Angeles, CA 90024.
† To whom requests for reprints should be sent at the above address.
‡ Division of Orthopedic Surgery, UCLA School of Medicine.
§ Department of Orthopedic Surgery, University of Southern California, School of Medicine, Los Angeles, California.

TABLE 1
MRI Appearance of Bone and Soft Tissue

Tissue	Signal intensity	
	T1-weighted	T2-weighted
Cortical bone	Black	Black
Fibrocartilage		
Ligaments & tendons		
Fat (including fatty marrow)	White	White (but < T1)
Muscle	Intermediate	Intermediate
Articular cartilage		
Acute hematoma		
Low-protein fluid	Black	White
High-protein fluid	White	White
Subacute hematoma		
Chronic hematoma	Black	Black
Inflammation	Intermediate	White
Tumor		

The patients were positioned supine, with their feet in a comfortable degree of plantarflexion to minimize patient motion. We found this position to be better tolerated in older patients than prone scanning, which has also been used.[7] A sagittal scout image was performed, and the coronal and axial planes were identified from the scout. In Figure 1A, the planes used are shown, designated as sagittal, coronal, or axial.

Normal anatomy was identified from anatomic texts,[5,12] with comparisons to cadaveric cryosections and gross dissection. We have performed more than 100 scans of the foot and ankle in the past 2 years. Of these cases, six were chosen to exemplify situations in which we found MRI to be particularly useful. Evaluation of the abnormal cases was done with full knowledge of clinical data and results of other imaging modalities.

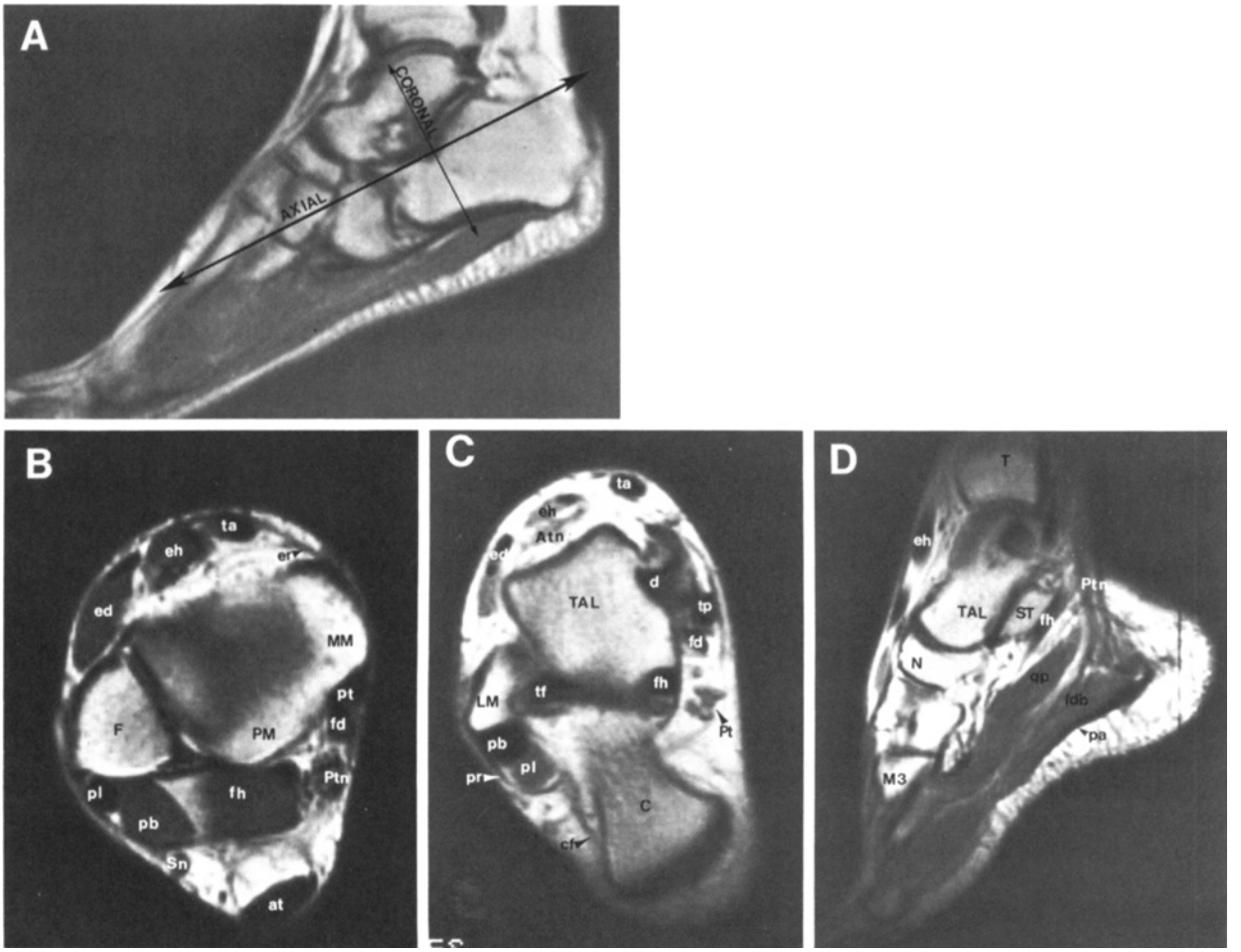

Fig. 1. Normal anatomy seen on MRI, T1-weighted (TE28/TR300-800). *A*, Sagittal scout, with axial and coronal planes marked. *B*, Axial, medial malleolus. *C*, Axial, lateral malleolus. *D*, Sagittal, middle subtalar facet. *E*, Sagittal, posterior and anterior subtalar facets. *F*, Sagittal, peroneus longus and brevis. *G*, Coronal, posterior subtalar facet. *H*, Coronal, middle subtalar facet. *I*, Coronal, anterior subtalar facet. Abbreviations: AF, anterior facet subtalar joint; ah, abductor hallucis; am, abductor digiti minimi; at, Achilles tendon; Atn, anterior tibial neurovascular bundle; C, calcaneus; cf, calcaneofibular ligament; CU, cuboid; d, deltoid ligament; ed, extensor digitorum longus; edb, extensor digitorum brevis; eh, extensor hallucis longus; er, extensor retinaculum; F, fibula; fd, flexor digitorum longus; fdb, flexor digitorum brevis; fh, flexor hallucis longus; il, interosseous ligament; LM, lateral malleolus; lp, long plantar ligament; Lpn, lateral plantar neurovascular bundle; M, metatarsal; MF, middle facet

Confirmation of diagnosis was made either by surgery or clinical follow-up.

RESULTS

In Figure 1, B–I, normal anatomy of the sagittal, coronal, and axial planes of the foot is seen. Because many of the structures of the foot are small and may not be identifiable in all planes, the figure provides a guide for optimal scanning in different clinical situations.

In Figures 2 through 7, cases in which MRI contributed significantly to diagnosis are seen.

CASE REPORTS

Case 1

A 41-year-old woman, after right ankle fusion, had a chronic ulcer of the dorsum of the right foot adjacent

Fig. 1.

subtalar joint; MM, medial malleolus; Mpn, medial plantar neurovascular bundle; N, navicular; pa, plantar aponeurosis; pb, peroneus brevis; pl, peroneus longus; PF, posterior subtalar facet; PM, posterior malleolus; Pr, peroneal retinaculum; Ptn, posterior tibial neurovascular bundle; qp, quadratus plantae; s, spring ligament; Sn, sural nerve & saphenous vein; ST, sustentaculum tali; T, tibia; ta, tibialis anterior; TAL, talus; tf, talofibular ligament; tp, tibialis posterior; TS, tarsal sinus.

to a calcaneal staple. An MRI was performed to evaluate for possible osteomyelitis (Fig. 2, A and B). Despite metal artifact from the arthrodesis (arrows), a focal marrow abnormality (arrowhead) within the calcaneus was well seen. In this case, the characteristic findings of osteomyelitis are shown: low-signal intensity in T1-weighted images and high-signal intensity with T2-weighting.[11] Infection was confirmed with open biopsy and culture.

Case 2

A posterior tibial tendon tear was clinically suspected in this 64-year-old woman. The T1-weighted MRI (Fig. 3) showed an enlarged tendon sheath filled with intermediate signal intensity (arrow), but a small area of low-signal intensity consistent with intact tendon fibers was discernible (arrowhead). This correlated precisely to the findings at surgery, where a nearly complete tear, sparing a single strand of intact tendon, was seen.

Case 3

A 38-year-old man was referred to us with a diagnosis of suspected giant-cell tumor. Radiographs revealed expansion and increased radiolucency of the medial tibia (Fig. 4A). Several years previously, he had undergone open reduction and internal fixation of a medial malleolar fracture. An MRI was performed, using phase contrast spin echo sequences (Fig. 4B) to enhance any marrow abnormality, in addition to conventional spin echo sequences. With the phase contrast sequence, abnormal marrow would show low signal. No abnormality was present on any of the sequences in the region where tumor was suspected. A healed fracture line (arrowhead) and a bone infarct (arrow) at the site of a previous screw were seen.

Case 4

A 53-year-old obese woman complained of a painful ankle mass that had slightly increased in size during a

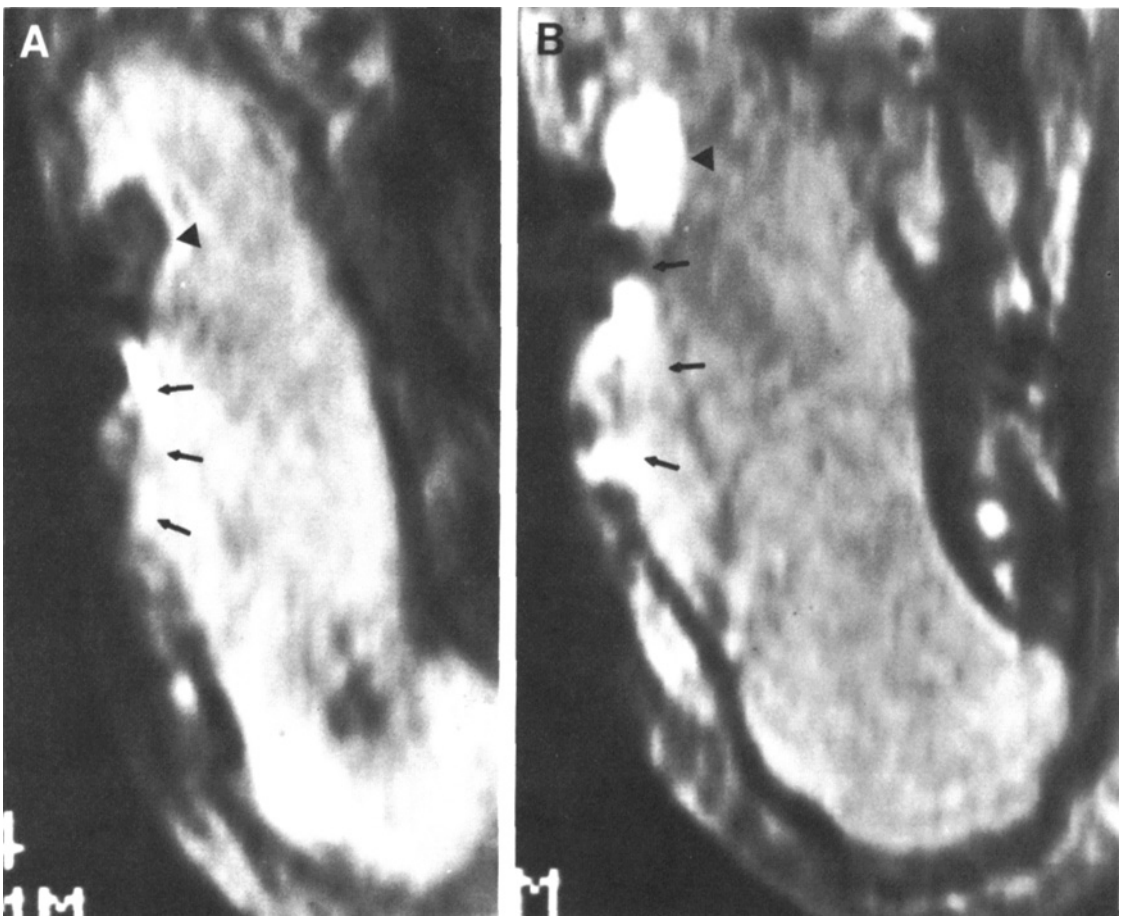

Fig. 2. Case 1, osteomyelitis after arthrodesis. *A*, Axial MRI, T1-weighted (SE 28/778). *B*, Axial MRI, T2-weighted (SE 56/2000).

Fig. 3. Case 2, posterior tibial tendon rupture, axial MRI (SE 28/556).

year's time. Physically, the mass could not be separated from the Achilles tendon. MRI (Fig. 5) showed an enlarged Achilles tendon of abnormally high signal intensity. Discontinuity of tendon fibers was seen anteriorly (arrow). In our experience, MRI of complete Achilles tendon rupture shows retraction of the tendon superiorly, with the area of tendon rupture filled with fat from the pre-Achilles space. This scan was therefore thought to show a partial rather than a complete tendon rupture. The patient's pain resolved with bed rest.

Case 5

MRI was performed on an 11-year-old girl several weeks following debridement of osteomyelitis of the distal fibula (Fig. 6, A and B). Abnormally low-signal intensity, which did not cross the physis, was present in the marrow. Thick periosteal new bone was also present (arrow). Within the low-signal area was a small region of signal void consistent with dense calcification in a sequestrum (Fig. 6B, arrowhead). A sequestrum was faintly visible on radiographs. The patient left the country and was lost to follow-up.

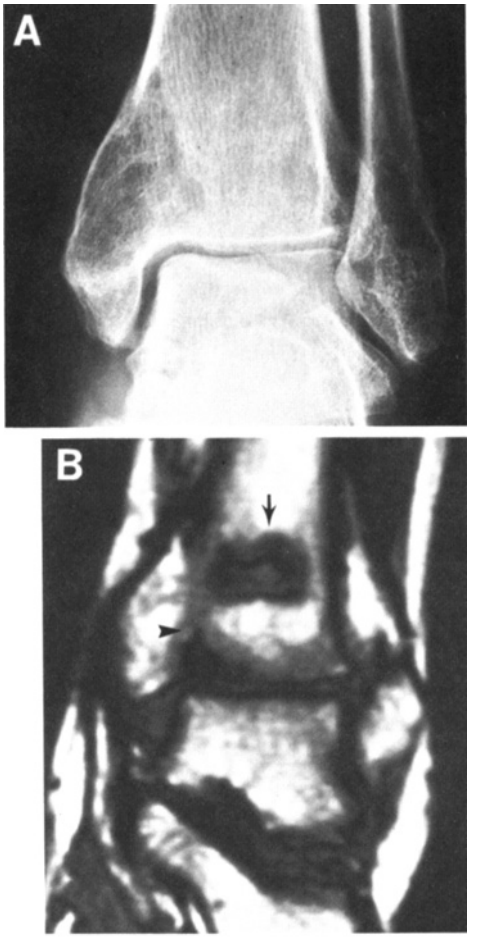

Fig. 4. Case 3, suspected giant cell tumor. *A*, AP radiograph of ankle. *B*, Coronal MRI, SE phase contrast.

Case 6

A 26-year-old woman, after open reduction and internal fixation of a talar neck fracture, complained of ankle pain. Radiographically (Fig. 7A), osteoarthritis of the tibiotalar joint was seen and questionably increased density of the talar dome. MRI (Fig. 7B) showed an area in the talar dome where high-signal fat was surrounded by a low-signal band (arrow). This is one of the characteristic MRI appearances of avascular necrosis.[1] Metal artifact (arrowhead) is from screw.

DISCUSSION

The clarity and soft-tissue detail of MRI enable a vivid understanding of the three-dimensional anatomy of the foot that is invaluable in studying this region. Clinically, we have found it to be useful in the evaluation of ligamentous and tendonous injuries, soft tissue masses, avascular necrosis, osteomyelitis, and other bone marrow abnormalities.

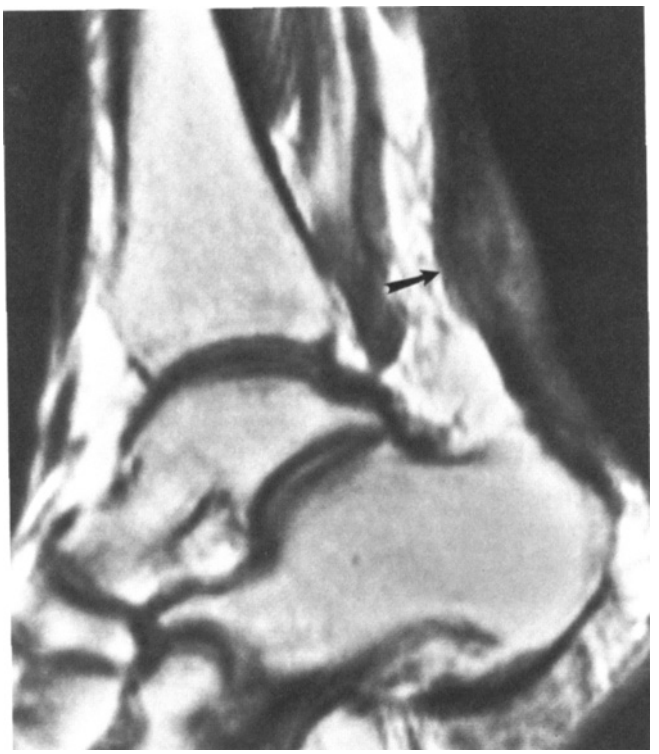

Fig. 5. Case 4, chronic, incomplete Achilles tendon rupture, sagittal MRI (SE 28/300).

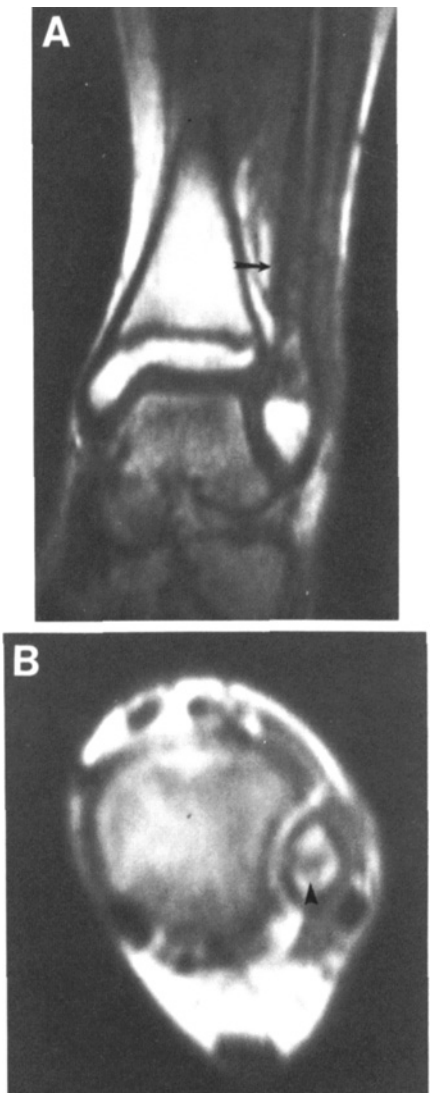

Fig. 6. Case 5, osteomyelitis. *A*, Coronal MRI, T1-weighted (SE 28/277). *B*, Axial MRI, T1-weighted (SE 28/500).

Although the soft tissues of the foot can be evaluated on CT,[9] the individual ligaments and tendons tend to appear blended with other, adjacent soft tissue. Also, differentiation between normal and abnormal tissue can be difficult. On MRI, injury to ligaments and tendons will result in an increased signal within the structure (cases 2 and 4). Plantar fasciitis, for example, would show intermediate signal in the normally black plantar aponeurosis. Calcaneal spurs without fasciitis, in contrast, are black (cortical bone) and sometimes contain marrow (white).

The long plantar and spring ligaments, important in maintaining the arches of the foot, can be evaluated, although we have not yet used this capability clinically. The origin and extent of soft tissue masses can be assessed (case 4).

We have commonly identified arthritis and joint effusions on MRI, but we believe that MRI has little to add to the radiograph in these conditions.

Bone marrow abnormalities are detected with great sensitivity (cases 1, 3, 5, and 6). Osteomyelitis can be distinguished from cellulitis[11] and avascular necrosis can be diagnosed before it is clinically evident.[1]

Disruption of the posterior facet in calcaneal fracture can be identified on MRI, but CT is more useful clinically in these fractures because it can show small fragments of cortical bone that may not be visible with MRI. This drawback of MRI occurs because cortical bone is black, as are ligaments and tendons, so that if the normal anatomic relationships are disrupted these tissues may be impossible to distinguish. MRI is, however, useful in evaluating secondary injury to the peroneal tendons in calcaneal fractures.

MRI is also useful in assessing the success of an arthrodesis of the ankle or hindfoot, because when osseous union is present, there is continuity of high-signal marrow between bones.

In low-field strength magnets, evaluation can often be successful despite the presence of metallic fixators, but as field strength increases, metal artifact becomes more prominent and may preclude visualization of the joint.[9] We have frequently, although not invariably, obtained diagnostic scans in patients who had a variety of metallic devices (cases 1 and 6).

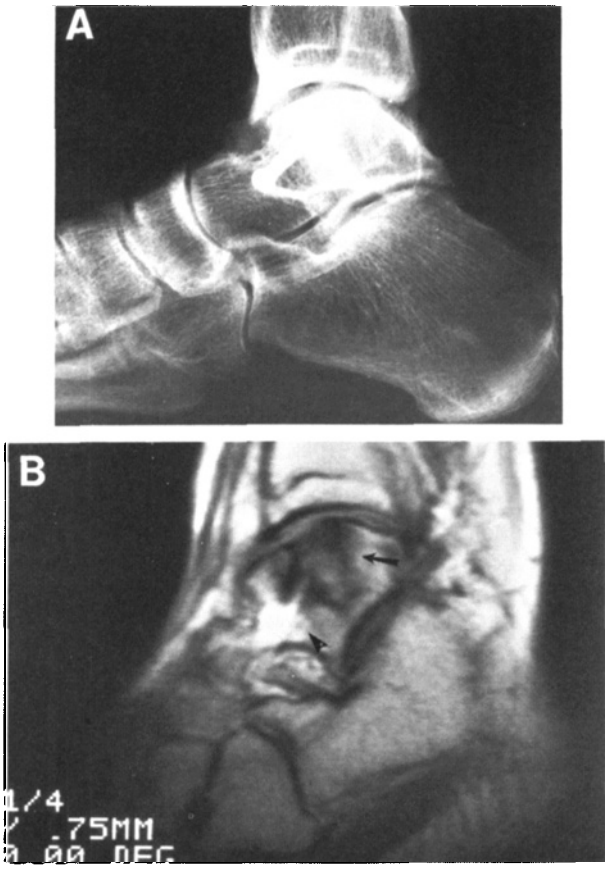

Fig. 7. Case 6, osteonecrosis of the talus. *A*, Lateral radiograph of the foot. *B*, Sagittal MRI, T1-weighted (SE 28/500).

REFERENCES

1. **Bassett, L. W., Gold, R. H., Reicher, M., Bennett, L. R., and Tooke, S. M.**: Magnetic resonance imaging in the early diagnosis of ischemic necrosis of the femoral head. Preliminary results. Clin. Orthop., **214:**237–248, 1987.
2. **Beltran, J., Noto, A. M., Herman, L. J., and Lubbers, L. M.**: Tendons: high-field strength, surface coil MR imaging. Radiology, **162:**735–740, 1987.
3. **Beltran, J., Noto, A. M., Mosure, J. C., Shamam, O. M., Weiss, K. L., and Zuelzer, W. A.**: Ankle:surface coil MR Imaging at 1.5T. Radiology, **161:**203–209, 1986.
4. **Hajek, P. C., Baker, L. L., Bjorkengren, A., Sartoris, D. J., Neumann, C. H., and Resnick, D.**: High-resolution magnetic resonance imaging of the ankle: normal anatomy. Skeletal Radiol., **15:**536–540, 1986.
5. **McMinn, R. M. H., Hutchings, R. T., and Logan, B. M.**: Color Atlas of Foot and Ankle Anatomy. Norwalk, CT, Appleton Century Crofts, 1982.
6. **Sartoris, D. J., and Resnick, D.**: Magnetic resonance imaging of podiatric disorders: a pictorial essay. J. Foot Surg. **26:**336–350, 1987.
7. **Sartoris, D. J., and Resnick, D.**: Magnetic resonance imaging of the foot: technical aspects. J. Foot Surg., **26:**351–358, 1987.
8. **Sartoris, D. J., and Resnick, D.**: Pictorial review: cross-sectional imaging of the foot and ankle. Foot Ankle, **8:**59–80, 1987.
9. **Solomon, M. A., Gilula, L. A., Oloff, L. M., and Oloff, J.**: CT scanning of the foot and ankle:2. Clinical applications and review of the literature. Am. J. Roentgenol. **146:**1192–1203, 1986.
10. **Stark, D. D., and Bradley, W. G.** Magnetic Resonance Imaging. St. Louis, CV Mosby, 1988.
11. **Tang, J. S. H., Gold, R. H., Bassett, L. W., and Seeger, L. L.**: Musculoskeletal infection of the extremities: evaluation with MR imaging. Radiology, **166:**205–209, 1988.
12. **Warwick, R., and Williams, P. L.**: Gray's Anatomy, 35th British Ed. Philadelphia, W.B. Saunders, 1973.